Sewage Outfall Plume Mapping using a Least Squares Collocation Method

Patrícia Ramos [1], Sérgio Cunha [2]

Keywords

Least squares collocation method, Mapping plume dispersion, Monitoring sewage outfalls, Autonomous Underwater Vehicles

Introduction

Several monitoring campaigns, with different spatial and temporal resolutions, have been used to study particular components of wastewater, their dispersal and impacts. However, the sewage outfall plume mixing process in coastal waters has continued to be a difficult problem to study *in situ* ([5]).

In general, the results of the field studies performed in order to detect and map sewage plumes using different types of techniques show very complex and patchy structures, both in vertical and horizontal sections, difficult to identify with the classic picture of the buoyant plume ([1,2,3,4,5,7,8,9]).

As advanced by several investigators ([3,2,5,8,9]), the observed plume patchiness can be due to one or a combination of factors which include: (1) variations in currents and stratification during time intervals, which can be hours in some cases, separating the beginning and the end of the field tests, that may result in different equilibrium depths or even distinct plume behaviours; (2) internal tides that can result in the effluent undergoing significant vertical excursions as it advects from the outfall; (3) limitations of sampling in terms of resolution of time and space scales; in reality field measurements are not truly synoptic since the time required for, e.g., a transverse of several kilometres can last a couple of hours; (4) inadequate numbers of critical variables, in particular, spatial and temporal aliasing and undersampling.

Rapid sampling is then expected to reduce time and space variability during and between transects ([10,11]). Because of their easier field logistics, reduced cost per study, increased spatial coverage, reduced spatial aliasing effects, and adaptive sampling capabilities, Autonomous Underwater Vehicles (AUVs) are especially attractive to detect and map sewage plumes ([6]).

Our focus is upon the use of a REMUS (Remote Environmental Measuring UnitS) AUV to measure physical properties of an outfall plume in order to characterize dispersion in the near field.

Isurus REMUS AUV (Figure 1) was acquired to the Woods Hole Oceanographic Institution, MA, USA in 1997. These vehicles are low cost, lightweight AUVs specially designed for coastal waters monitoring ([12]). The reduced weight and dimensions makes them extremely easy to handle, requiring no special equipment for launching and recovery.

Isurus has a diameter of 20 cm and is about 1.5 meters long, weighting about 35 kg in air. The maximum forward speed of the vehicle is 4 knots, however the best energy efficiency is achieved at about 2 knots. At this velocity, the energy provided by a set of rechargeable Lithium-Ion batteries may last for over 20 hours (i.e., over 40 nautical miles).

Although small in size, this vehicle can accommodate a wide range of oceanographic sensors,

[1] Patrícia Ramos, Mrs., PhD/Assistant, Department of Mathematics of Institute of Accountancy and Administration of Porto, Rua Jaime Lopes Amorim, s/n, 4465-004 S. Mamede Infesta, Portugal- +351.22.9050000 - patricia@iscap.ipp.pt. Faculty of Engineer of University of Porto, Ocean Systems Group, Institute of Systems and Robotics – Porto, Rua Dr. Roberto Frias, s/n, 4200-465 Porto, Portugal - +351.22.5081860 - patricia@fe.up.pt, URL: http://oceansys.fe.up.pt/.

[2] Sérgio Cunha, Mr, PhD/Assistant Professor, Faculty of Engineer of University of Porto, Rua Dr. Roberto Frias, s/n, 4200-465 Porto, Portugal - +351.22. 225081508 - sergio@fe.up.pt.

according to mission objectives. For the field experiment described in this paper three specific sensors were integrated: a CTD (Conductivity, Temperature, Depth), OS200 model from Ocean Sensors, USA, a Light Scattering Sensor, from WETLabs, Inc. and an altimeter, from Imagenex, Canada.
There are two data sets collected during a typical mission. The first set is related to the vehicle internal data, which is only analysed in the laboratory. This allows to evaluate the performance of the various subsystems (navigation, control, power consumption, etc) and provide useful information for potential improvements. The other data set comprise all the information from the oceanographic sensors.

Figure 1 – *Isurus* Autonomous Underwater Vehicle.

The *S. Jacinto* outfall is located on the Portuguese west coast near *Aveiro* region. It's total length, including the diffuser, is 3378 m (the first 3135 m with a diameter of 1600 mm and the last 243 m with a diameter of 1200 mm). The diffuser, consisting of 72 ports alternating on each side, 0.175 m diameter, is 332.52 m long. Currently, only the last 20 of the 72 ports are working in a length of 98.16 m. These are discharging upwards at an angle of 30° above the horizontal axis, being the port height about 1.3 m.
The outfall has a true bearing direction of 290° and is discharging at a varying depth approximately between 14 and 17 m. The sea floor near the diffuser has a moderate sloping sandy bottom with isobaths oriented parallel to the coastline. In that zone the coastline itself runs at about a 200° angle with respect to true north.
In this paper we briefly describe a monitoring mission to study the shape of the *S. Jacinto* outfall plume using *Isurus* AUV performed on July 2002. The steps followed in data processing to map the dispersion using a Least Squares Collocation Method (LSCM) technique are fully described.

AUV Monitoring Mission

One of the major problems related to the plume tracking studies is the sampling plan ([11]). In order to reduce the uncertainty about plume location and concentrate the vehicle mission only in the hydrodynamic mixing zone, outputs of RSB (Roberts-Snyder-Baumgartner) near field prediction model ([13]), based on effective real time *in situ* measurements of current speed and direction and density stratification, were opportunistically used to specify in real time the mission transects ([6]).
The near field plume predictions, including, length of hydrodynamic mixing zone, spreading width at the end of the near field, maximum rise height, and thickness, defined the AUV 3D survey area.
With current direction, these spatial limits were used for the adaptive placement of the sampling transects to optimally sample the plume.
The AUV monitoring mission to *S. Jacinto* outfall took about 1 hour and 52 minutes, starting approximately at 14:00 GMT. A rectangular area of 200x100 m^2 starting 20 m downstream from the middle point of the diffuser was covered (see in Figure 2 the vehicle position estimate in blue color).
As predicted, the vehicle performed trajectories in 6 horizontal sections at 2, 4, 6, 8, 10, and 12 m depth. In each horizontal section, the vehicle described 6 parallel transects perpendicular to the water current direction, of 200 m long spaced of 20 m.
During the mission, the vehicle transited horizontally and vertically at a constant velocity of approximately 1 m/s (i.e., aprox. 2 knots). Data were recorded at a rate of 2.4 Hz, so horizontal resolution was about 0.4 m (we define horizontal resolution as the approximated distance between consecutive points that are sampled at the same depth). Vertical resolution varied along the mission

due to the natural currents influence on the vehicle navigation but was almost always between 1-2 m (we define vertical resolution as the vertical distance between points in the water column that are sampled approximately at the same (X,Y) location but at consecutive depths).
Optical backscattering data were highly promising for the plume mapping, at least to be used in combination with temperature and salinity. Unfortunately, the sensor was not correctly tuned in terms of gain signal, so the measurements obtained could not be used.

Data Processing
In order to effectively map the dispersion of the effluent using the AUV data three main steps were followed.
In the first step, after a global analysis to the collected data (where, for example, errors due to sensor malfunctions were detected), an estimate of the trajectory described by the vehicle more suited for spatial location of the oceanographic data gathered was produced and then CTD and navigation data were merged onto a common time base using linear interpolation.
Positioning data were then rotated about -3.86° so that North-South/East-West lines were aligned with *x*-*y* axis.
In the second step, using the polynomials developed by [14], in situ conductivity, temperature and pressure were used to compute salinity. Then, density was estimated by using this computed salinity and the measured temperature and pressure.
Finally, the last step was to plot the desired variables onto *x*-*y*, *x*-*z*, and *y*-*z* grids using Least Squares Collocation Method (LSCM) technique ([15]). The LSCM has been used for numerous applications namely for the numerical solution of differential equations such as the Navier-Stokes equations, and hyperbolic problems, including the shallow water equations, to interpolate gravity at any given location using only measurements at some discrete locations, etc.
To apply Least-Squares Collocation Method, we first chose a finite set of $N = 396$ collocation points:

$$\{X_j\}_{j=1,\ldots,396} = \{\{-90:20:110\},\{-120:20:-20\},\{2:2:12\}\}, \quad (1)$$

in the measurements domain $\Omega = [-98,118]\times[-125,3]\times[1,13]$.

Figure 2 – AUV plume tracking survey and collocation points: (a) plan view; (b) 3D plan

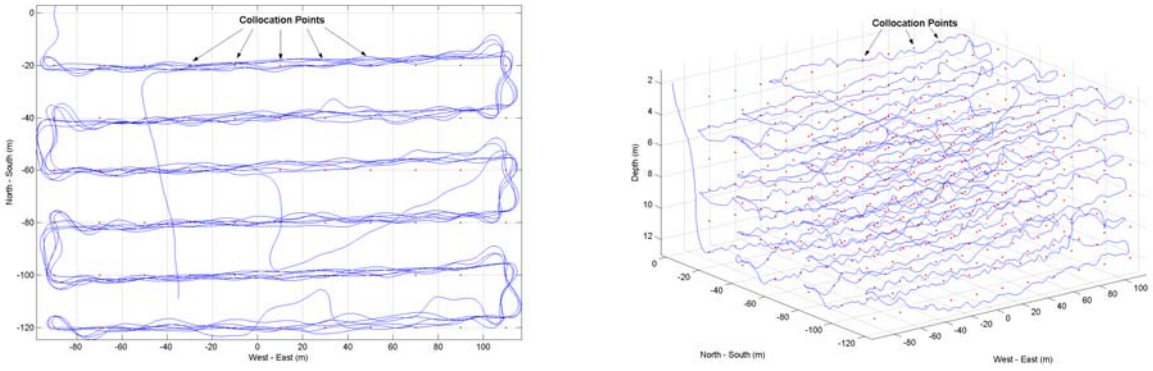

Then we assumed an approximation of the desired variable (in this case, salinity, temperature and density, denoted here by *P*) between measured and collocation points in the form:

$$P_i \approx \sum_{j=1}^{N} W_{ij}\hat{P}_j, \quad i = 1,\ldots,n \Leftrightarrow P = W\hat{P}, \quad (2)$$

where P_i is the measurement at point X_i, with $n = 16075$ observations, $\hat{P}_j$ represents the approximated measurement at collocation point X_j, and W_{ij} is an elementary function usually built in such a way that it takes a certain value if X_i is in the influence domain of point X_j, the region Ω_j, and vanishes outside the region Ω_j surrounding the point X_j. W is a n by N matrix ($n > N$)

where the column vector j represents the magnitudes of the approximated measurement of collocation point X_j with respect to each observation i, and where the row vector i represents the magnitudes of the approximated measurements of each collocation point X_j with respect to observation point X_i.

Our choice for the elementary function W_{ij} was the following raised cosine function:

$$W_{ij}(d) = \begin{cases} \frac{1}{2} + \frac{1}{2}\cos(\pi d), & 0 \le d < 1 \\ 0, & d \ge 1 \end{cases}, \tag{3}$$

where d is a normalized distance given by:

$$d(X_i, X_j) = \left\| X_i - X_j \right\|_{nrm} = \left[\left(\frac{|x_i - x_j|}{\Delta x} \right)^{nrm} + \left(\frac{|y_i - y_j|}{\Delta y} \right)^{nrm} + \left(\frac{|z_i - z_j|}{\Delta z} \right)^{nrm} \right]^{\frac{1}{nrm}}, \tag{4}$$

being $nrm = 2.45$, $X_i = (x_i, y_i, z_i)$, $X_j = (x_j, y_j, z_j)$ and $\Delta x = 20$, $\Delta y = 20$, and $\Delta z = 2$ the cell grid distances respectively in x, y and z axis, between consecutive collocation points.

Note that if X_i is in the influence domain of point X_j, the value W_{ij} is as large as less distanced are the points X_i and X_j, being a unit value when $X_j = X_i$ (and null for all the other collocation points).

Since the magnitudes are constants, Equation (2) is an overdetermined linear system of equations (n equations with N unknowns) which can be solved using least squares method, by one of the several mathematical packages such as *Matlab*, the one used in our case.

Note that the least squares functional is defined by summing the squares of the residuals evaluated for each point X_i:

$$J = \sum_{i=1}^{n} \left[P_i - \sum_{j=1}^{N} W_{ij} \hat{P}_j \right]^2 = \left(P - W\hat{P} \right)^T \left(P - W\hat{P} \right). \tag{5}$$

Minimization of (5) with respect to $\hat{P}$ leads to:

$$\left(W^T W \right) \hat{P} = W^T P, \tag{6}$$

where W^T is the transpose of matrix W. Solving the resulting system (of N equations with N unknowns) for $\hat{P}$ we obtain:

$$\hat{P} = \left(W^T W \right)^{-1} W^T P. \tag{7}$$

An important advantage of this method is the sparsity of the matrix W. Since W has a high percentage of zero-valued elements, using a sparse matrix data only the nonzero elements and their indices are stored, reducing significantly the amount of memory for storage, and making the matrix inversion calculation process more efficient. Only a few seconds were necessary for the matrix inversion process, being W a 16075 by 396 matrix.

Notice that d was not defined exactly as Euclidean distance, i.e. L_2 norm, but a $L_{2.45}$ norm. The explanation for this is illustrated in Figure 3: plots (a) and (b) show the behavior of function W for a 1D measurement domain $\Omega = [0,4]$, and collocation points $\{X_j\}_{j=1,2,3} = \{1,2,3\}$ with $\Omega_1 = [0,2]$, $\Omega_2 = [1,3]$, and $\Omega_3 = [2,4]$; plots (c), (d), and (e) show the behavior of function W for a 2D measurement domain $\Omega = [0,3] \times [0,3]$, and collocation points $\{X_j\}_{j=1,2,3,4} = \{(1,1),(2,1),(1,2),(2,2)\}$ with $\Omega_1 = [0,2] \times [0,2]$, $\Omega_2 = [1,3] \times [0,2]$, $\Omega_3 = [0,2] \times [1,3]$, and $\Omega_4 = [1,3] \times [1,3]$ using L_2 norm, and plots (f), (g), and (h) are the

same as before except using $L_{2.45}$ norm.

Figure 3 – Behavior of weight function W for a 1D and a 2D measurement domain, using norm L_2 and $L_{2.45}$ in 2D case.

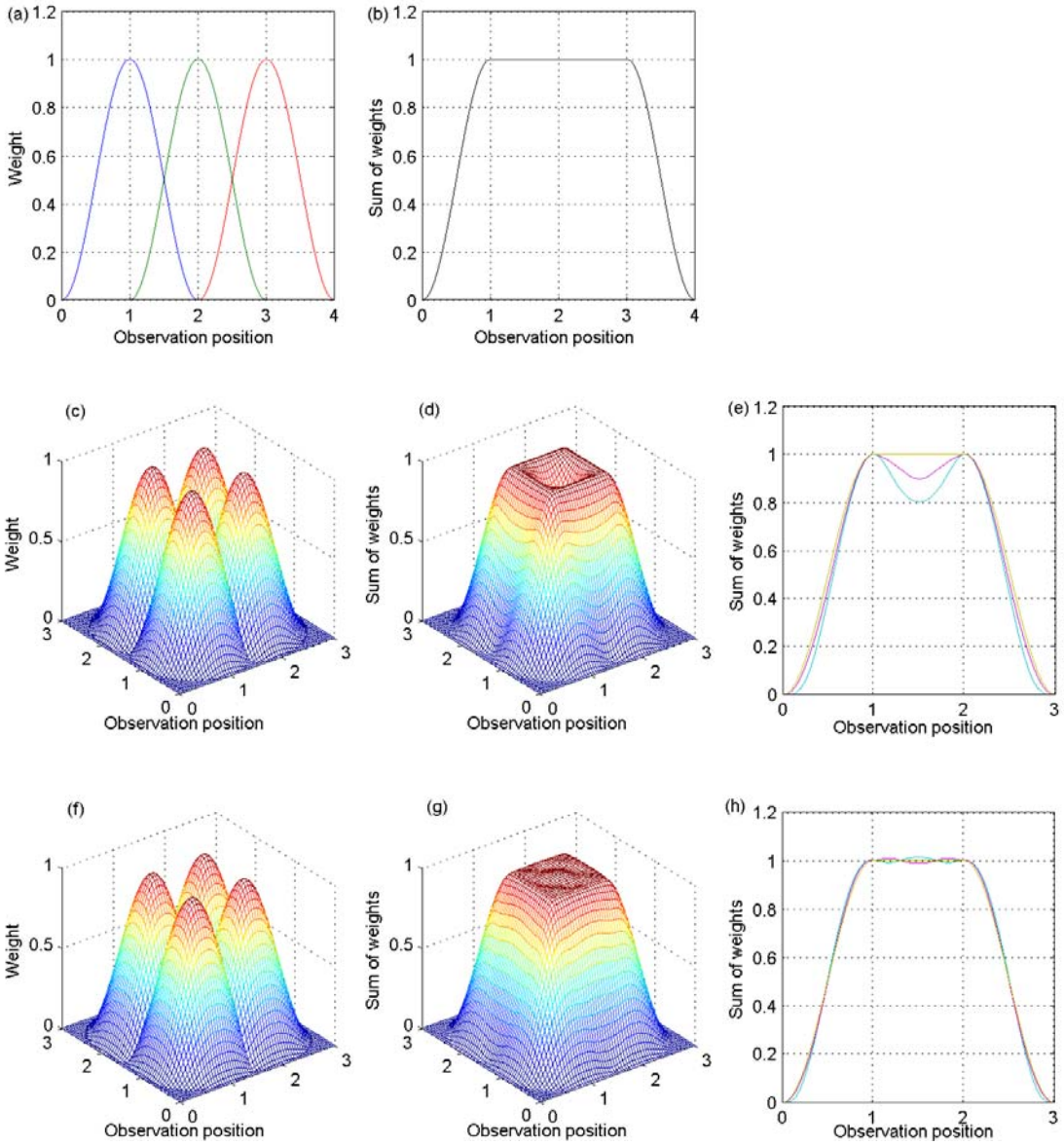

As can be seen from plot (b), in the 1D measurement domain case, the sum of magnitudes of the approximated measurements of each collocation point X_j with respect to a observation point X_i, with $d = |x_i - x_j|$ in the influence domain of point X_j is, as expected, a unit value, except in the boundaries of course.

In the 2D measurement domain case, as can be seen from plot (d) and (e), the sum of magnitudes of the approximated measurements of each collocation point X_j with respect to a observation point X_i, with $d = \sqrt{|x_i - x_j|^2 + |y_i - y_j|^2}$, the Euclidean distance, in the influence domain of point X_j, is not as should, a unit value, except of course in the boundaries. This problem is partially eliminated if a

norm $L_{2.45}$ is used, as show plots (g) and (h). This value was empirically adjusted so that the sum of magnitudes of the measurements of each collocation point be approximated a unit value. Cross sections for the 3D measurements domain case (not shown) were performed and the results are similar to the 2D case previously presented.
A "less visited collocation point"' X_j was defined as one whose sum of magnitudes (sum of elements of column vector j) was less then the difference between the mean value of the all sums of magnitudes (SumMag) and three times the standard deviation of these sums:

$$lessvisit_j = \sum_{i=1}^{n} W_{ij} < \left(mean(\text{SumMag}) - 3 \times std(\text{SumMag})\right). \quad (8)$$

To increase information on the desired variable in the vicinity of less visited collocation points X_j, a cell grid size update was performed:

$$\left[\Delta x\, \Delta y\, \Delta z\right]_j = \text{cell\_growth} \times \left[\Delta x\, \Delta y\, \Delta z\right]. \quad (9)$$

where $\text{cell\_growth} = 5$.
Finally, a finer meshgrid of the form $\left[\Delta x\, \Delta y\, \Delta z\right] = \left[2\ 2\ 0.2\right]$ was considered for the visualization surface generation. The desired variable on the M visualization points was calculated as follows:

$$\tilde{P}_k = \sum_{j=1}^{N} \tilde{W}_{kj} \hat{P}_j + mean(P), \quad k = 1, \ldots, M, \quad (10)$$

were the weights matrix $\tilde{W}_{kj}$ was evaluated in the same manner as (3). To improve the method efficiency, the least squares solution (7) was either computed as follows:

$$\hat{P} = \left(W^T W\right)^{-1} W^T \left(P - mean(P)\right), \quad (11)$$

so the mean value has to be added in (10).
Several interpolation methods such as Nearest Neighbor, Bilinear, and Bicubic were first applied to the measured data but with no successful results. The LSCM was then considered since it is specially attractive for problems posed on irregularity shaped domains, which is the case
here. Giving the intermittence of the phenomena in observation, using "local" functions instead of using elementary functions which cover the all measurements domain (e.g., Fourier Series), no influence is assumed between widely estimated measurements of the desired variable.

Results and Discussion

Similarly to other field studies ([1,5,7]) salinity was found to be more useful than either temperature or density in observing the plume structure.
The LSCM results for salinity parameter are presented in Figure 5. This figure shows salinity longitudinal sections, West-East, between -20 and 100 m, with 20 m spacing. Temperature results (not presented) do not give a clear picture of the plume structure. Although not so significant, density results (also not presented) show some similarity with salinity ones.
From this figure it is possible to identify unambiguously the effluent plume and observe its evolution downstream. It appears as a region of lower salinity compared to surrounding ocean waters at the same depth, rising to the water surface due probably to the weak stratification and relatively low currents. It is also possible to observe the plume edges since the wastefield width is shorter than the survey width.
The plume spreading direction agrees quite well with the measured currents. South from the diffuser (downstream), evidence of sewage effluent at the surface continued, with lower salinities than that observed at the edges of the sections. Salinity differences compared with the surrounding waters at the surface started to be about 0.4 psu within a distance of 20-40 m from the diffuser, decreasing to about 0.15 psu at a distance of 40-60 m, being less than 0.1 psu at 100 m distance from the diffuser, and ending almost equally to background waters at 120 m distance.

Salinity anomalies in the plume compared to background waters at the same depth range of the same order were found by [1] and [5]. Vertical profiles of salinity collected by [5] at the center or over the western end of the diffuser, where the highest effluent concentrations were found, indicated differences of 0.2 psu. Typical salinity anomalies in the plume, of the order of -0.1 psu were observed by [1].
The effluent plume was detected from nearly the surface (at minimum depths around 1.5 m) to nearly 8 m depth within a distance of 20-80 m from the diffuser, clearly decreasing thickness downstream. A sharp difference in salinity at the effluent plume lateral edges is clearly visible, being the wastefield spreading almost centered in the survey area.
This indicates that the sampling strategy designed was successful even for a surfacing plume that can be considered as the most complicated case in terms of natural tracer tracking. A surfacing plume, several times more diluted than a submerged plume, surrounded by low salinity surface waters, with its own weak signals, could be further blurred by the background signals.
The plume exhibits a considerably more complex structure than the compact shape of the classical picture of the buoyant plume, but not so patchy as in previous studies [2,3,4,8,9], maybe due to the improvements in horizontal and vertical resolution ([6]) and also possibly to the LSCM results, which removed high frequency fluctuations, providing a better estimate of the averaged salinity.
According to laboratory experiments with diffuser orientation perpendicular to a steady current of uniform density [13], when the current Froude number *F* is greater than 1, which is the case here, the plume mixes with the current throughout the water depth while is carried downstream. This is known as a forced entrainment region where the current becomes too large for the plume to entrain all the incoming flow and maintain the free plume pattern, becoming attached to the lower boundary. Except for the lower boundary attachment, since no salinity variations were found at least at 12 m depth, this plume behavior seems to be in agreement with the observed results.

Figure 5 – Longitudinal sections of salinity (psu) results.

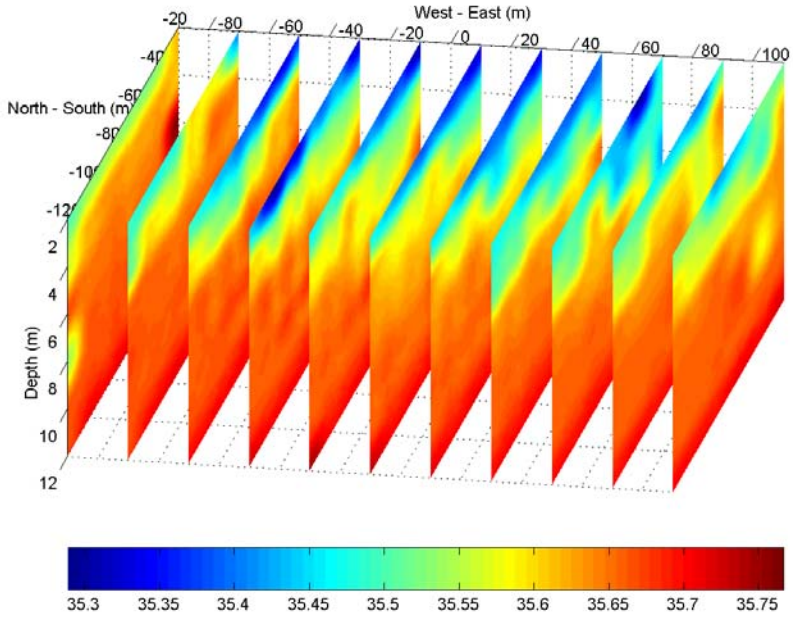

Conclusions

An oceanographic campaign was performed on July 2002 to study the shape of *S. Jacinto* sewage plume using *Isurus* AUV. Our results demonstrate that AUVs can provide high-quality measurements of physical (and probably optical) properties of effluent plumes in a quite effective manner.
An efficient sampling strategy, enabling improvements in terms of resolution of time and space scales and undersampling, demonstrated that sewage effluent plumes can be clearly traced using naturally occurring tracers in the wastewater. In order to reduce the uncertainty about plume

location and concentrate the vehicle mission only in the hydrodynamic mixing zone, outputs of a near field prediction model, based on *in situ* measurements of current speed and direction and density stratification obtained in real-time, were used to specify the AUV mission.

A data processing system was created, applying the Least Squares Collocation Method (LSCM) technique, in order to effectively map the dispersion of the effluent using the AUV data. LSCM results for salinity enable to identify unambiguously the effluent plume and observe its dispersion downstream. The effluent plume appears as a region of lower salinity compared to surrounding ocean waters at the same depth, rising to the water surface probably due to the weak stratification and relatively low currents.

The use of artificial tracers would probably provided even more rigorous measurements than the natural tracers temperature and salinity. However, since our method is considerably less expensive and more practical for routine monitoring, not forgetting the negative impacts of releasing fluorescent dyes or other traceable components in the effluent, further developments in the future will certainly be conducted.

References

[1] Washburn, L., Jones, B. H., Bratkovich, A., Dickey, T. D., Chen, M.: "Mixing, dispersion, and resuspension in vicinity of ocean wastewater plume", Journal of Hydraulic Engineering, ASCE, 118, (1), pp. 38-58, 1992.

[2] Carvalho, J.L.B., Roberts, P.J.W. and Roldão, J.: "Field Observations of the Ipanema Beach Outfall", Journal of Hydraulic Engineering, ASCE 128(2), 151–160, 2002.

[3] Faisst, W.K., McDonald, R.M., Noon, T. and Marsh, G.: "Iona Outfall, Plume Characterization Study", In Proceedings 1990 National Conference on Hydraulic Engineering, ASCE, H. Chang, New York, San Diego Ed, 1990.

[4] Wu, Y., Washburn, L., Jones, B. H.: "Buoyant plume dispersion in a coastal environment: evolving plume structure and dynamics", Continental Shelf Research, 14, (9), pp. 1001-1023, 1994.

[5] Petrenko, A. A., Jones, B. H., Dickey, T. D.: "Shape and initial dilution of sand island, Hawaii sewage plume", Journal of Hydraulic Engineering, ASCE, 124, (6), pp. 565-571, 1998.

[6] Ramos, P.: "Advanced mathematical modeling for outfall plume tracking and management using autonomous underwater vehicles based systems", PhD Thesis, FEUP, 2005.

[7] Jones, B.H., Barnett, A. and Robertson, G.L.: "Towed Mapping of the Effluent Plume from a Coastal Ocean Outfall", In Conference Proceedings MTS-IEEE Oceans 2001, MTS 0-933957-29-7, 1985-1989, 2001.

[8] Hunt, C.D., Steinhauer, W.S., Mansfield, A.D., Albro, C.A., Roberts, P.J.W., Geyer, W.R. and Mickelson, M.J.: "Massachusetts Water Resources Authority Effluent Outfall Dilution: April 2001", Boston, Massachusetts Water Resources Authority. Report ENQUAD 2002-06, 69 p. plus appendices, 2002.

[9] Hunt, C.D., Mansfield, A.D., Roberts, P.J.W., Albro, C.A., Geyer, W.R., Steinhauer, W.S. and Mickelson, M.J.: "Massachusetts Water Resources Authority Effluent Outfall Dilution: July 2001", Boston, Massachusetts Water Resources Authority. Report ENQUAD 2002-07, 77 p., 2002.

[10] Ramos P., Neves M.V., Cruz N. and Pereira, F.L.: "Outfall Monitoring Using Autonomous Underwater Vehicles", In Proceedings of MWWD2000 – Marine Waste Water Discharges International Conference 2000, Genova, Italy, 2000.

[11] Ramos P., Cruz N., Matos, A., Neves M.V. and Pereira, F.L.: "Prediction Studies for an AUV Monitoring Mission Plan", In Fifth International Conference on the Mediterranean Coastal Environment, Medcoast 2001, Hamammet, Tunisia, pp. 1299-1310, 2001.

[12] Alt, C.V., Allen, B., Austin, T. and Stokey, R.: "Remote Environmental Measuring Units", In Proceedings of the Autonomous Underwater Vehicles '94 Conference, 1994.

[13] Roberts, P.J.W., Snyder, W.H. and Baugartner, D.J.: "Ocean Outfalls. Parts I, II, and III", Journal of Hydraulic Engineering, ASCE, 115(1), 1-70, 1989.

[14] Millero, F.J., Chen, C.T., Bradshaw A., Schleicher, K.: "A New High Pressure Equation of State for Seawater", Deep-Sea Research, 27A, pp. 255-264, 1980.

[15] Zhang, Xiong, Liu, Xiao-Hu, Song, Kang-Zu, Lu, Ming-Wan: "Least-Squares Collocation Meshless Method", International Journal for Numerical Methods in Engineering, Vol. 51, pp. 1089-1100, 2001.

Patrícia Alexandra Gregório Ramos obtained her licenciate degree in Applied Mathematics – Field of Computer Science from Faculty of Sciences of University of Porto in 1993, Master degree in Electrical and Computer Engineering- Field of Systems from Faculty of Engineer of University of Porto (FEUP) in 1996 and PhD in Engineering Sciences from FEUP in 2005. She is Teaching Assistant at the Department of Mathematics of Institute of Accountancy and Administration of Porto, Polytechnic School of Porto. Her research activity is carried out in the Ocean Systems Group of Institute for Systems and Robotics at FEUP, in the areas of fluid mechanics associated to transport and mixing of pollutants, monitoring of coastal waters and diffusion phenomena, assessment and management of sea outfalls, environmental impact studies of sewage outfall discharges and Underwater Autonomous Vehicles.

Sérgio Cunha obtained his licenciate degree in Electrical and Computer Engineering from FEUP in 1991, Master degree in Electrical and Computer Engineering- Field of Systems from FEUP in 1994 and PhD in Electrical and Computer Engineering from FEUP in 2001. He is Assistant Professor at the Department of Electrical and Computer Engineering of FEUP. Some of his research areas include linear and nonlinar control, optimal control, stochastic control, robust control, system estimation, semidefinite programming, etc.

Faculty of Engineer of University of Porto
Rua Dr. Roberto Frias, s/n 4200-465 Porto PORTUGAL